University of Baghdad
College of Engineering
JE
JOURNAL OF ENGINEERING

Journal of Engineering

journal homepage: www.jcoeng.edu.iq

Volume 30 Number 5 May 2024

Orbital Prosthesis Rehabilitation in Biomedical Engineering by Means of Computer Vision-Photogrammetry and 3D Prototyping

Mohammed R. Falih [1,*], Fanar M. Abed [1, 2]

[1] Department of Surveying Engineering, College of Engineering, University of Baghdad, Baghdad, Iraq
[2] Honorary member of the University of Exeter, Exeter, UK
mohammed.r@coeng.uobaghdad.edu.iq[1], fanar.mansour@coeng.uobaghdad.edu.iq[2]

ABSTRACT

Eye loss may be caused as a result of eye trauma, accidents, or malignant tumors, which leads the patient to undergo surgery to remove the damaged parts. This research examines the potential of computer vision represented by Structure from Motion (SfM) photogrammetry in fabricating the orbital prosthesis as a noninvasive and low-cost technique. A low-cost camera was used to collect the data towards extracting the dense 3D data of the patient facial features following Structure from Motion-Multi View Stereo (SfM-MVS) algorithms. To restore the defective orbital, a Reverse Engineering (RE) based approach has been applied using the similarity RE algorithms based on the opposite healthy eye to rehabilitate the defected orbital precisely. Following quality assurance and best-fitting statistical analysis, the digital model of the restored eye was converted into a physical model using 3D prototyping. This is later used to fabricate the mold for casting medical-grade silicone to obtain the final orbital prosthesis. The results show the power of SfM photogrammetry by offering a high-accuracy model of 0.048 mm and 0.186 mm relative errors acquired in the horizontal and vertical directions, respectively. These results boost the RE implementation in medicine to reconstruct the patient's damaged eye by mirroring the image of the healthy eye using RE algorithms. Therefore, the margin matching results claim perfect data capture settings and successful data processing workflow as designed in the first place. Consequently, one can claim this approach effectively rehabilitates maxillofacial deformities as an alternative to invasive restoration approaches. The presented approach provided a low-cost and safe workflow that avoids the patient the risks of exposure to harmful rays or magnetic fields available in other sensors.

Keywords: Biomedical, SfM-MVS photogrammetry, Virtual restoration, Rapid prototyping, Maxillofacial rehabilitation.

*Corresponding author
Peer review under the responsibility of University of Baghdad.
https://doi.org/10.31026/j.eng.2024.05.01
This is an open access article under the CC BY 4 license (http://creativecommons.org/licenses/by/4.0/).
Article received: 16/10/2023
Article accepted: 17/04/2024
Article published: 01/05/2024

إعادة تأهيل الأطراف الاصطناعية المدارية في الهندسة الطبية الحيوية باستخدام المسح التصويري القائم على الرؤية الحاسوبية والنماذج الأولية ثلاثية الأبعاد

محمد رحمن فالح[1,*]، فنار منصور عبد[2,1]

[1] قسم هندسة المساحة, كلية الهندسة, جامعة بغداد, بغداد, العراق

[2] جامعة إكستر، إكستر، المملكة المتحدة

الخلاصة

قد يحدث فقدان العين نتيجة لصدمة بالعين أو حوادث أو أورام خبيثة مما يدفع المريض إلى إجراء عملية جراحية لإزالة الأجزاء التالفة. في هذا البحث، تم فحص إمكانيات الرؤية الحاسوبية متمثلاً بالمسح التصويري القائم على الهيكل من الحركة (SfM) في تصنيع الطرف الاصطناعي المداري كتقنية غير جراحية ومنخفضة التكلفة. تم استخدام كاميرا منخفضة التكلفة لجمع البيانات من اجل استخراج البيانات الثلاثية الأبعاد الكثيفة لملامح وجه المريض باتباع خوارزميات الهيكل من الحركة - استريو متعدد الرؤية (SfM-MVS). لاستعادة المدار المعيب، تم تطبيق النهج القائم على الهندسة العكسية (RE) باستخدام خوارزميات التشابه RE المستندة إلى العين السليمة المقابلة لإعادة تأهيل المدار المعيب بدقة. وبعد اتباع ضمان الجودة والتحليل الإحصائي الأفضل، تم تحويل النموذج الرقمي للعين المستعادة إلى نموذج مادي باستخدام النماذج الأولية ثلاثية الأبعاد، والتي يتم استخدامها لاحقًا لتصنيع قالب لصب السيليكون الطبي للحصول على الطرف الاصطناعي المداري النهائي. أظهرت النتائج قوة المسح التصويري القائم على الهيكل من الحركة (SfM) من خلال تقديم نموذج عالي الدقة يبلغ 0.048 مم و0.186 مم من الأخطاء النسبية المكتسبة في الاتجاهين الأفقي والرأسي على التوالي. تعمل هذه النتائج على تعزيز تطبيق الهندسة العكسية في الطب لإعادة بناء عين المريض المتضررة من خلال عكس صورة العين السليمة باستخدام خوارزميات الهندسة العكسية. ولذلك، فإن نتائج مطابقة الهامش تتطلب إعدادات مثالية لالتقاط البيانات وسير عمل معالجة البيانات الناجح كما تم تصميمه في المقام الأول. لذلك، يمكن القول أن هذا النهج قدم فعالية في إعادة تأهيل تشوهات الوجه والفكين كحل بديل لأساليب الترميم. يوفر النهج المعروض سير عمل منخفض التكلفة وآمنًا يجنب المريض مخاطر التعرض للأشعة الضارة أو المجال المغناطيسي المتوفر في أجهزة الاستشعار الأخرى.

الكلمات المفتاحية: الطب الحيوي، المسح التصويري SFM-MVS، الترميم الافتراضي، النماذج الأولية السريعة، إعادة تأهيل الوجه والفكين.

1. INTRODUCTION

The eye is the mirror of the soul, not just for vision, but also plays a significant role in a person's facial expression and personality **(Sharma et al., 2014; Nalawade et al., 2013; Pun et al., 2016)**. Eye loss is rarely congenital **(Goiato et al., 2018; Maskey et al., 2019; Singh et al., 2019)** but can usually be acquired as a result of cancer, trauma, sympathetic ophthalmia, or blind eye pain **(Jamayet et al.,2013; Shrivastava et al., 2015; Lanzara et al., 2019; Maskey et al., 2019)**. In most cases, eye loss results from malignant tumors surrounding the eye or internal tumors extending outside the eye. Where a surgical intervention is performed to eradicate these tumors, and thus all the contents of the eye are

removed, including the eyelids, extraocular muscles, fat, optic nerve, and lacrimal gland. The postsurgical outcome is a bare orbital cavity **(Bali et al., 2015; Weisson et al., 2020)**. The loss of an eye is physically and psychologically distressing to the patient and can severely affect human interactions **(Sharma et al., 2014; Karayazgan-Saracoglu and Ozdemir, 2017; Cevik and Kocacikli, 2019; Weisson et al., 2020).** Orbital prostheses significantly rehabilitate patients with unilateral orbital defects **(Buzayan et al., 2015; Liu et al., 2019)**. These prostheses improve the patient's life, enhance self-confidence, improve the external appearance, and preserve the anatomical structures after surgical treatment **(Alam et al., 2017; Ballo et al., 2019; Gachake et al., 2021)**. Artificial eyes date back to ancient times, where the earliest known examples of mummies date back to the Fourth Dynasty in Egypt (1613-2494 BC) **(Sharma et al., 2014)**. Fabrication of maxillofacial prostheses using traditional impression techniques has many drawbacks, including (i) causing deformation of the facial topography surface due to the pressure or the weight of the impression material **(Matsuoka et al., 2019)**, (ii) methods are costly and time-consuming and require technicians' skills for sculpting and painting **(Salazar-Gamarra et al., 2016; Yadav et al., 2017)**, (iii) the sensitivity of the materials used, (iv) the difficulty of dealing with the materials as it requires experience and training, especially when working in an environment that affects the interaction of the used materials, and (v) when the defects are large in the face, this requires covering the entire face, which may cause suffocation of the patient. Further, using a cannula to facilitate breathing from the mouth can distort the tissues of the face, causing an impression to be distorted **(Salazar-Gamarra et al., 2016)**. Recently, advanced digital technologies have enabled us to obtain accurate external measurements and 3D-anatomic models and it represents the best choice to address this problem by creating a digital impression. Computer-Aided-Design / Computer-Aided-Manufacturing (CAD/CAM) technique provided a new approach to fabricating maxillofacial prosthetics **(Ballo et al., 2019)**. Acquired 3D data from patients can be achieved with several methods such as Computed Tomography (CT), Magnetic Resonance Imaging (MRI), 3D laser technique, or others (i.e. computer vision photogrammetry technique) **(Chunhua and Guangqing, 2020).** Computed Tomography (CT) and Magnetic Resonance Imaging (MRI) represent the most popular methods for data acquisition **(Chiu et al., 2017)**. Although the CT scan or MRI provides accurate 3D data for the soft tissues **(Ballo et al., 2019)**, it exposes the patient to a large amount of radiation and magnetic field **(Chiu et al., 2017)**. Therefore, laser or photographic scanning represents an alternative solution to eliminate the effect of this radiation. With digital development, prostheses can be fabricated in a record time, which may reach a few hours by integrating different technologies such as CAD design, Reverse Engineering, and Rapid prototyping. Additionally, it is important to acknowledge that developments in processing techniques have integrated laser technology with smartphones as low-cost LIDAR sensors **(Abbas and Abed, 2024)**. It also can provide opportunities to collect accurate data measurements and get a digital impression of the facial area.

Advanced technologies have been employed by many researchers. **(Ciocca and Scotti, 2014)** carried out a study to improve the manufacturing process of the orbital prosthesis through the combination of MRI technology and laser scanning to collect patient data. The researchers have stated that MRI enables the user to obtain accurate details of soft tissues compared to a CT scan and that laser scanning will give accurate details of the face surface in record time compared to the traditional method. The authors suggested using the M1-class of the laser beam for safety scanning. In another study, **(Liu et al., 2019)** suggested using two different scanners for facial digitizing. A facial laser scanner can obtain general facial topography and an intraoral scanner to get more details healthy eye, then fusion the

two data scanning to fabricate an appropriate orbital prosthesis. The clinical outcome was satisfactory and effective in time and effort spent compared to the traditional methods. The scholars reported details obtained by the intraoral scanner can reach the required accuracy in fabricating textures of surface skin. One of the problems with using intraoral laser scanning in facial digitizing is the difficulty of restoring alignment loss because the facial topography is flatter than teeth. To solve this problem, the scans can use reference points **(Salazar-Gamarra et al., 2016).**

Other alternative techniques had to be introduced to overcome the radiation and magnetic field risks that may be posed to the patient due to using CT-Scan or MRI. **(Reitemeier et al., 2004)** suggested using a 3D-photogrammetry system (Kolibri-mobile: IVB) to (i) eliminate the risks of radiation and magnetic field exposure when CT and MRI scanning were used and (ii) Reduce the stress experienced by the patient when using traditional methods. **(Bi et al., 2013)** suggested that for misrepresentation prevention in data acquisition, the scan should be conducted at 45 degrees from left and right, and then the scan data should be merged using a CAD software suite. On the other hand, **(Salazar-Gamarra et al., 2016)** employed the photogrammetry technique to obtain a 3D model to digitally scan the face and be used later in maxillofacial rehabilitation using open-source software and a low-cost device (smartphone). Later, **(Chiu et al., 2017)** were the first whom describe the use of digital cameras to collect data from a patient to build a template for an orbital prosthesis. Images were taken at 1.5 meters with three different levels, and they used Autodesk 123D Catch, a 3D reconstruction open-source software, for processing the images and obtaining a digital model. Then to restore the damaged eye, they used Z-brush software by Pixologic Inc., USA. The researchers have found that this approach provides satisfactory results and minimizes the costs associated with data collection and modeling.

The previous highlighted studies used various sensors in data acquisition from the patient and did not only focus on photogrammetry in rehabilitating maxillofacial deformities. They also referred to alternative radiative and non-radiative remote sensing techniques for maxillofacial rehabilitation. However, photogrammetry has distinct advantages compared to other non-contact methods such as CT scans, MRIs, and portable laser scanning. To be more precise, photogrammetry allows for detailed impressions without causing discomfort or potential sensitivity to patients by processing the images captured and providing a 3D model of the deformable area. Compared to the costly tools and processes needed for CT and MRI scans, it is clear how economical photogrammetry is. With common cameras and software, photogrammetry becomes a more affordable and accessible choice; this is especially useful in resource-limited regions where advanced imaging technologies are not commonly available.

Therefore; this study aims to show the potential of the photogrammetric technique in fabricating the orbital prosthesis as a noninvasive and low-cost approach. The study investigated is based on inspecting the generated numerically based model using reference ground truth points placed in the background of the patient's head during the photo session. Additionally, providing the necessary photographic settings, developing the optimal capturing plan, and evaluating the generated model were considered to find how this technique is efficient for such applications and successfully contributes to the scientific society by providing a solid and sophisticated automatic digital routine in biomedical engineering. Section one introduces SfM photogrammetry in prosthesis rehabilitation and reviews relevant studies in this content. Section two illustrates the methodology implemented, including data capturing, processing, rehabilitation workflow, and analysis. The section also describes the patient case study. Section three presents analyses and

thoroughly discusses results following the virtual restoration and validation approach. Section four describes the conclusions delivered and section five highlights study limitations toward improvements in future prosthesis restoration studies.

2. METHOD

This study used the Close Range Photogrammetry (CRP) method to rehabilitate patients with maxillofacial deformities. The subsequent sections will detail the workflow implemented to achieve the optimal outcome for the required prosthesis.

2.1 Case Study

A 60-year-old female has lost her entire left eye socket due to a cancerous tumor. Fortunately, the patient's right eye is still functional since it was used to rebuild the missing eye using the RE approach.

2.2 Data Acquisition

Data acquisition represents an essential part of photogrammetry technology that significantly affects the accuracy of the results **(Abed, 2015; Difar and Abed, 2022)**. IPhone 11 Pro Max camera was used to acquire the facial data from the patient. IPhone camera sensor was chosen for collecting the data based on a previous image quality test conducted by the authors in a previous study **(Falih et al., 2021)**. The results show that the iPhone camera sensor delivers the best image quality. IPhone camera specification is illustrated in **Table 1.**

Table 1. The specification of iPhone 11 pro max camera.

Camera resolution	12
Sensor size (mm)	2.99 x 3.99
Camera Pixel size	0.991
Image resolution	4032 x 3024

Before image capturing, the patient was positioned with a stabilized head, remaining healthy eye open, and a normal expression. It should be noted that capturing more images from various locations is highly recommended in advanced photogrammetry solutions (i.e. SfM-MVS) because it leads to a robust network geometry. Therefore, reliable camera information and accurate object coordinates will be achieved **(Shamkhi and Abed, 2020)**. Furthermore, these extra images will be useful to gain a denser point cloud, leading to a more detailed object and increasing the model's resolution. Therefore, in this study, and based on image network calculations achieved by the authors in a previous study **(Falih et al., 2021)**, the image capturing was done using a 0.65 Base-to-height (B/H) ratio in the image network design with about 8 levels forming 4 main stations. Additionally, extra images were captured between these main stations, and about 37 images were captured closer to the patient's area of interest to get more details, leading to 102 images. The capturing scenario was from bottom to top in parallel lines similar to flight direction path lines (see **Fig. 1**). Coded targets with known coordinates have been placed in the patient's background as reference points for evaluating the generated model.

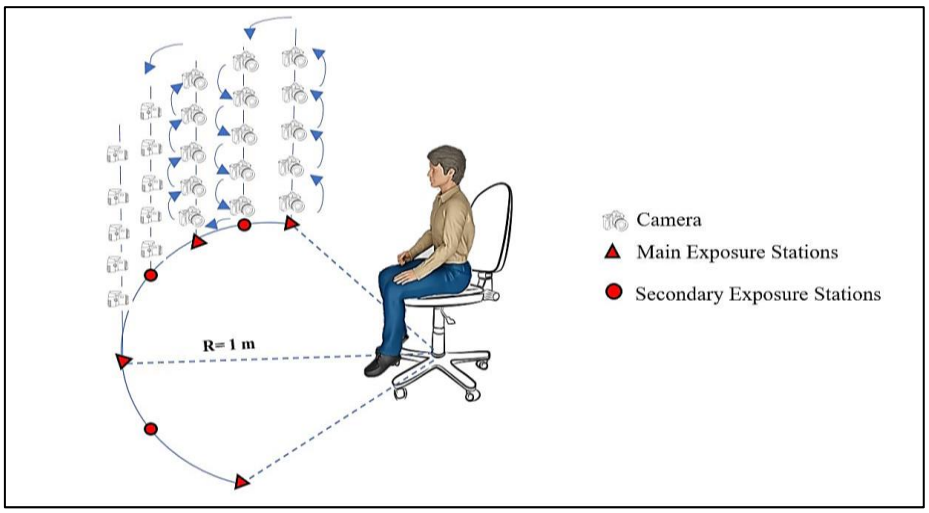

Figure 1. Capturing scenario.

2.3 Images Post-Processing

Metashape (Agisoft LLC, Russia) software has been used for processing the images, which is a commercial 3D reconstruction software. Metashape comes in Standard and Professional editions. This software runs on Windows, Mac OS, and Linux operating systems and provides a reliable and accurate model with precise texture by analyzing images and applying photogrammetry algorithms. This software is based on computer vision and applies the SfM algorithm to generate accurate 3D models from images **(Ahmed et al., 2022; Kloc et al., 2021; Sarhan and Abed, 2021)**. In Agisoft Metashape software, the photogrammetry workflow involves several steps, as shown in **Fig. 2.**

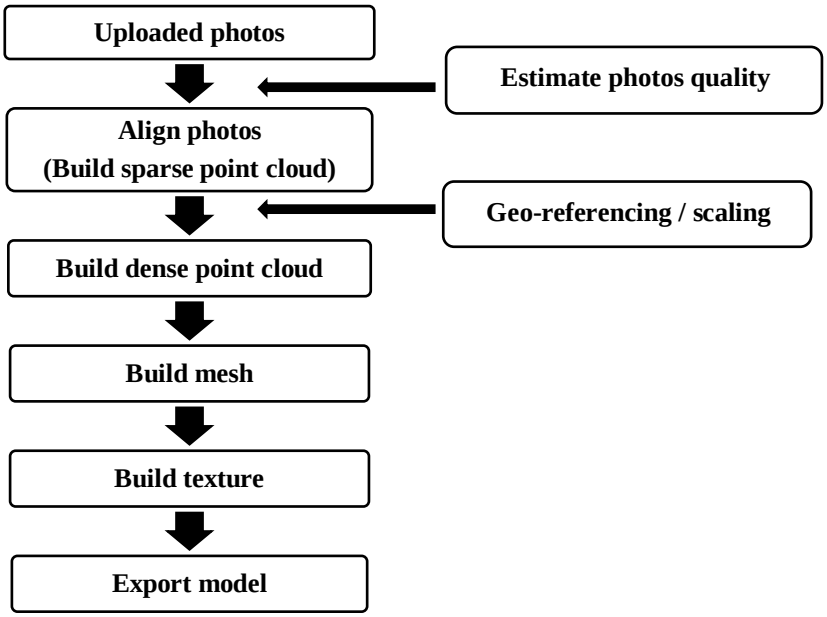

Figure 2. The general photogrammetry workflow in Metashape software.

The outcome model varies according to the model construction settings that are used. Metashape offers the capability to change these settings following the required accuracy. **Table 2.** shows the reconstruction settings used in this research.

Table 2. Reconstruction settings used in Metashape processing.

Processing steps	Reconstruction parameter	The selected settings	Description (Agisoft, 2021)
Align photo	**Accuracy:**	**Highest**	Help in obtaining accurate camera positions but at the expense of the time factor. In this setting, the software upscales the image by a factor of four (2 times on each side).
	Generic preselection:	**active**	Enables Metashape to run a quick pre-scan before starting full, common feature detection in a photo. This will help speed up the alignment process, especially when a large set of photos are uploaded.
	Reference pre-selection:	**deactivate**	This option is the best choice when only a few points are identified in the alignment stage.
	Key point limit:	**40000**	Indicates the maximum number of points to be extracted from each image
	Tie point limit:	**4000**	It represents the maximum number of points matched in each image.
Build Dense Point Clouds	**Accuracy:**	**Ultra-high**	This option provides more precise geometry than other options. However, it is a time–consuming workflow with Ultra high settings.
	Depth filtering:	**Aggressive**	This option allows deep filtering, so accurate geometry will be achieved.
	Calculate point color:	**Active**	The software will calculate the color for each point based on the images.
Build mesh	**Source data:**	**Dense cloud**	The dense point clouds that were previously generated will be used to create a high-quality mesh.
	Surface type:	**Arbitrary (3D)**	This option is suitable for modeling objects like sculptures, buildings, etc. However, the height field surface type suits planar surfaces, such as terrains, bas-reliefs, or aerial photography processes.
	Face count:	**High**	Specifies the maximum polygon count in the final mesh.
	Interpolation:	**Enabled (default)**	Enables interpolating surface area within a specified radius around each point of a dense cloud
Build texture	**texture type:**	**Diffuse map**	Represent the fundamental texture for storing the model's surface colors.
	source data	**Images**	The color texture map will be built based on aligned model photos.
	mapping mode	**keep uv**	This option specifies the texture packaging method for the object texture.
	Blending mode	**Mosaic (default)**	This option specifies combining the pixels' color values from different cameras.
	texture size/count	**4096**	The texture of the image pixel is wrapped on the mesh through this option.

2.4 Restoration Workflow

The restoration process is to reconstruct the damaged or missed part of an object and return it to its original state, depending on the remaining components of the object. Reverse Engineering (RE) technique is usually used in this process. This study used the RE technique to reconstruct the patient's damaged eye by mirroring the image of the healthy eye, as human eyes are largely symmetrical. **Fig. 3** shows the digital procedure followed.

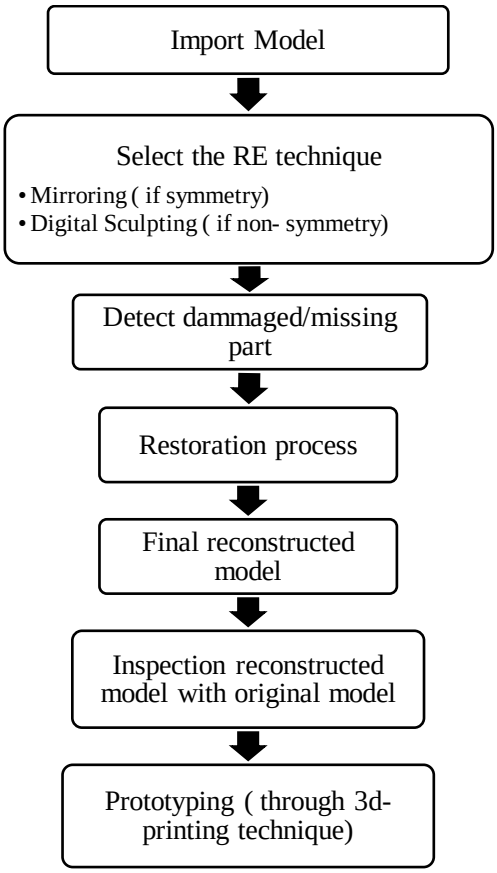

Figure 3. Typical digital restoration workflow.

2.4.1. Selected Software

3DReshaper was used to restore the missing part in the model by applying the RE technique. 3DReshaper is a simple and flexible software solution for processing any point cloud for various applications. It provides a comprehensive set of tools for 3D modeling and inspection requirements.

2.4.2. Detecting the Missing Parts

After model generating with Metashape, the next step is identifying the object's missing or damaged elements. As previously mentioned in section (2.1), the patient had a missing eye due to its surgical removal as a result of a malignant tumor (see **Fig. 4**). Fortunately, the patient's right eye is healthy, so it was mirrored to restore the missed eye by applying the reverse engineering technique.

Figure 4. Detect the missed part in the patient.

2.4.3. Virtual Restoration of Missed Eye

This study applied the restoration process based on the symmetry existing information (healthy eye). The general steps that were used can be illustrated as follows :

1- Planer symmetry was created in the middle patient's face to use it as a reference plane for the mirroring process.
2- The area of interest (missed eye area) has been extracted in reference and mirrored models, leaving sufficient overlap between them.
3- Applying the best-fit registration algorithm for obtaining best-fitting models.
4- Apply manual fitting using free-form deformation (FFD) to match the margins between the two models best.
5- The eye socket was offset by 2 mm inward and margins by 0.5 mm in the reference model to reduce the pressure of the prosthesis on the patient's eye socket and make it easy for our installation.
6- Merge the reference model, which will be the back of the prosthesis, with the mirror model, which will be the face of the prosthesis.
7- Increase the prosthesis thickness by 0.7 mm to maintain the prosthesis's durability .
8- Smooth the free border, but keep the details.
9- Export the final model for later printing preparation.

2.5. 3D-Printing of the Prosthesis

Following the restoration process, the restored model has been prepared for printing. Firstly, the model was imported in STL format in the Meshmixer software to check the model dimension, normal surface, and filling holes in the model. Although the Meshmixer software is used for printing preparation, it has limited capabilities, and it's not intended for resin printers. Therefore, another slicing software was used, chitubox v. 1.8.1. This software is a complete 3D printing preparation for editing and slicing the model. This software is intended for preparing models for printers that are curing the resin material to form solid 3D models. The Creality LD-002R LCD Resin 3d printer has been used to print the prepared model. The specifications of this printer are illustrated in **Table 3**. **Fig. 5** shows the final prepared model and the settings used.

Table 3. 3D printing specification

Modeling Technology	LCD
Print Size	119x65x160 mm
Print Speed	20-30 mm/h
Print support	Automatic/Manual
XY Axis Precision	0.075 mm
Package size	295x295x545 mm
Layer Height(quality)	0.01-0.05 mm
File Format	STL/CTB
Printing Material	Resin

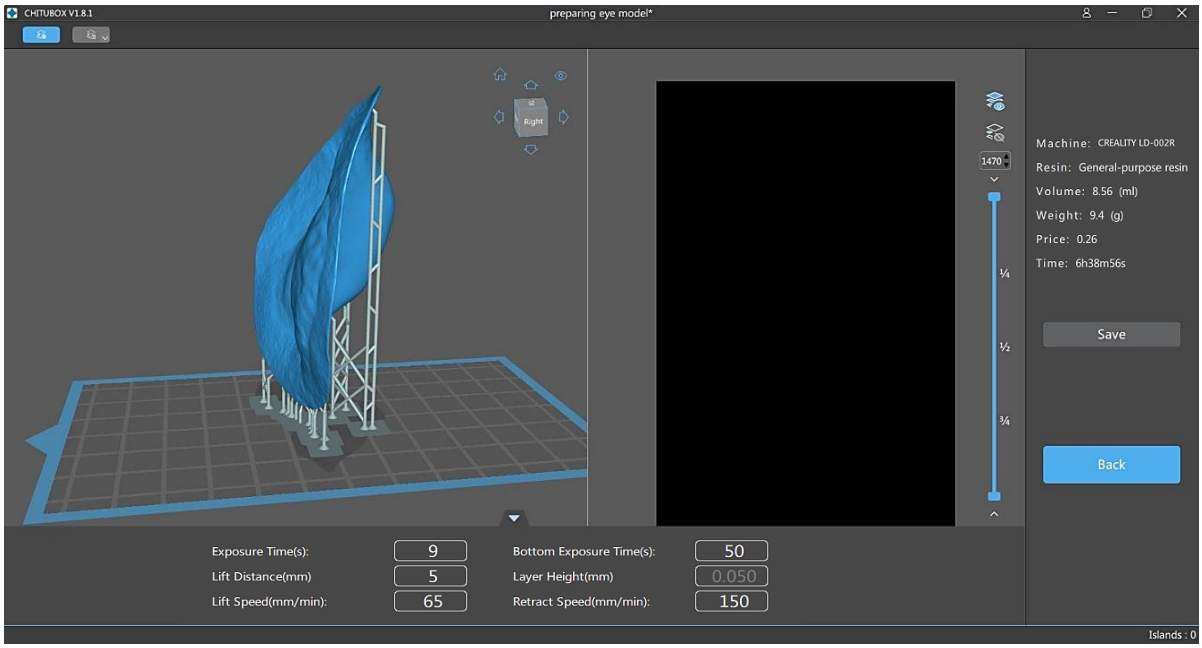

Figure 5. The final sliced 3D printed model.

3. RESULTS AND DISCUSSIONS

3.1. Data Processing

When uploading photos into the Metashape software, coded targets in source photos are detected automatically through the detect markers command in the tool menu. Then, the corresponding markers will be added to the Reference pane. Following that, the coordinates of these reference markers are uploaded. To validate the Metashape-based model, six reference points have been selected as control points (GCPs) and four as checkpoints. Then, the RMSE was calculated based on these references. The total errors for control and checkpoints were 0.144 mm and 0.198 mm, respectively. **Table 4**. shows the RMSE of checkpoints. After building the model in Metashape (alignment, building dense cloud, building mesh, and texture), post-processing steps were accomplished, and the model was generated, see **Fig. 6**.

Table 4. RMSE for checkpoints.

Label	X error (mm)	Y error (mm)	Z error (mm)	Total (mm)	Image (pix)
Check1	0.0706439	-0.0791900	0.1034170	0.1481780	0.832 (102)
Check2	0.0142822	0.0140259	-0.1732450	0.1743980	0.655 (84)
Check3	-0.0156024	-0.0162463	-0.1732140	0.1746720	0.947 (98)
Check4	0.0344233	-0.0746689	-0.2596590	0.2723660	0.75 (70)
Total	0.0406907	0.0554688	0.1858320	0.1981570	0.813

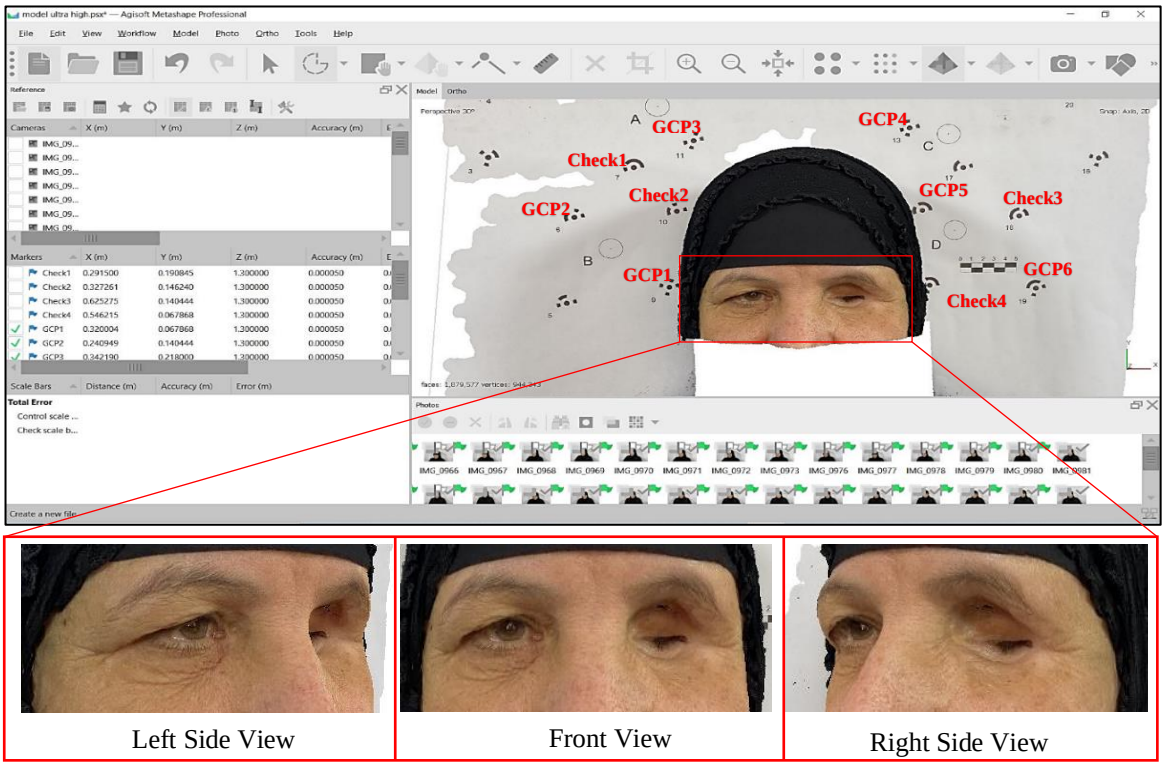

Figure 6. 3D textured models with the distribution of reference points.

From the result shown in **Table 4**, it can be noticed that the total error in the X-Coord. And the Y-Coord. were 0.041 mm and 0.055 mm, respectively. This is highly acceptable for such an application following previous relevant studies **(Salazar-Gamarra et al., 2016).** However, the total error in the Z-direction was 0.186 mm. This increment in error level in the Z-direction may have occurred due to the reference points selected for evaluation, as these have been erroneously targeted in approximately one depth value. This may affect the total root mean square error value estimated.

3.2. Virtual Restoration and Evaluation

The virtual restoration approach represents the best solution as an alternative to traditional methods that need much effort and are considered a time-consuming process, as well as need high skills sculpting technicians. In this study, after detecting the damaged part of the patient (the left eye), virtual restoration steps (as described in section (2.4.3)) have been applied, see **Fig. 7**.

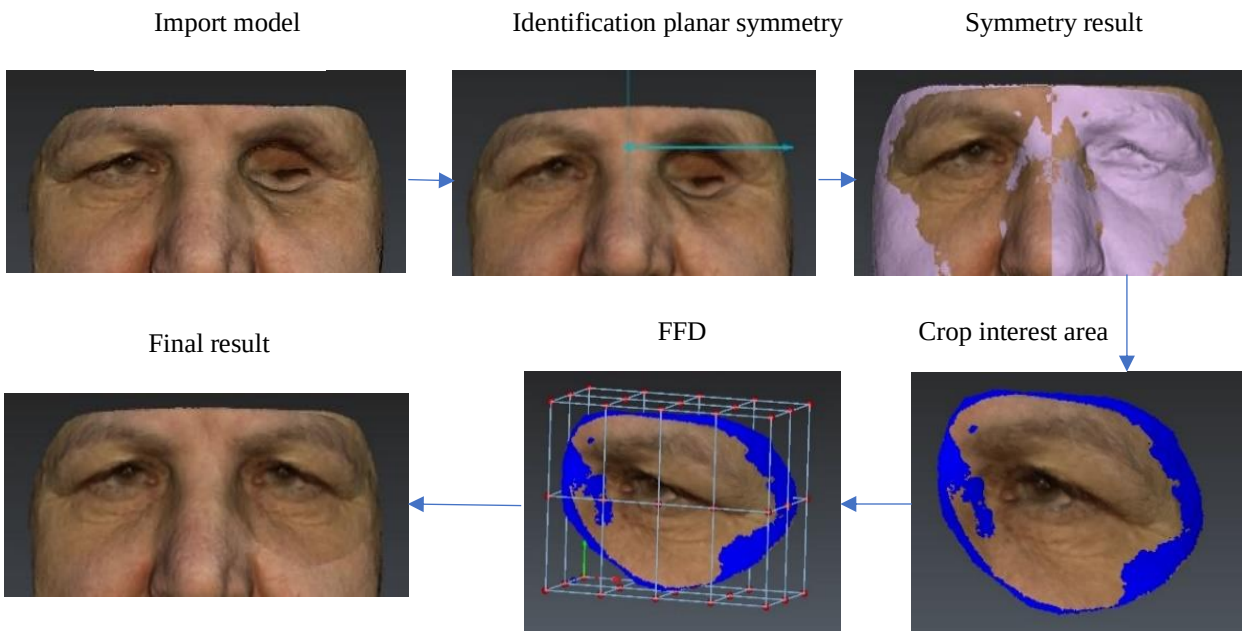

Figure 7. Virtual restoration pipeline.

In **Fig. 7**, it can be noticed that the half side of the patient model, which has the undamaged eye, was mirrored onto the contralateral side concerning the earlier identified planar symmetry. This symmetry confirms that half of the human face is not completely similar to the other side. Therefore, the restored eye model must be slightly modified for the best matching result.

Accordingly, it was necessary to evaluate the matching of the restored eye model with the original model, as digitally checking the fitting of the generated prosthesis on the patient's face is necessary, as it reflects the matching that can be obtained in reality. 3DResheper was used to inspect the restored model (prosthesis) with the original reference model. To ensure the restored model matches the reference model for inspection, the best-fit registration algorithm was used based on (0.96 mm) mean error and (1.62 mm) standard deviation. Then the (compare/inspect) function was implemented to obtain a color map showing how well the prosthesis matches the reference model, as shown in **Fig. 8**.

Through the results shown in **Fig. 8**, it can be noticed that the margins of the prosthesis illustrated in blue color were designed to obtain an actual match with the reference model. However, the eyebrow area illustrated in brown color has an error rate of approximately (1 mm). This is because the human eye is completely asymmetrical, meaning that when one eye is reversed, it does not fully match the other. Furthermore, the other errors illustrated in cyan, green, and red color range from (3 mm to 1 cm). This relatively considerable gap in the range is due to the absence of the eyelid and sclera in the reference model, hence, the difference in distances was calculated to the base of the eye socket.

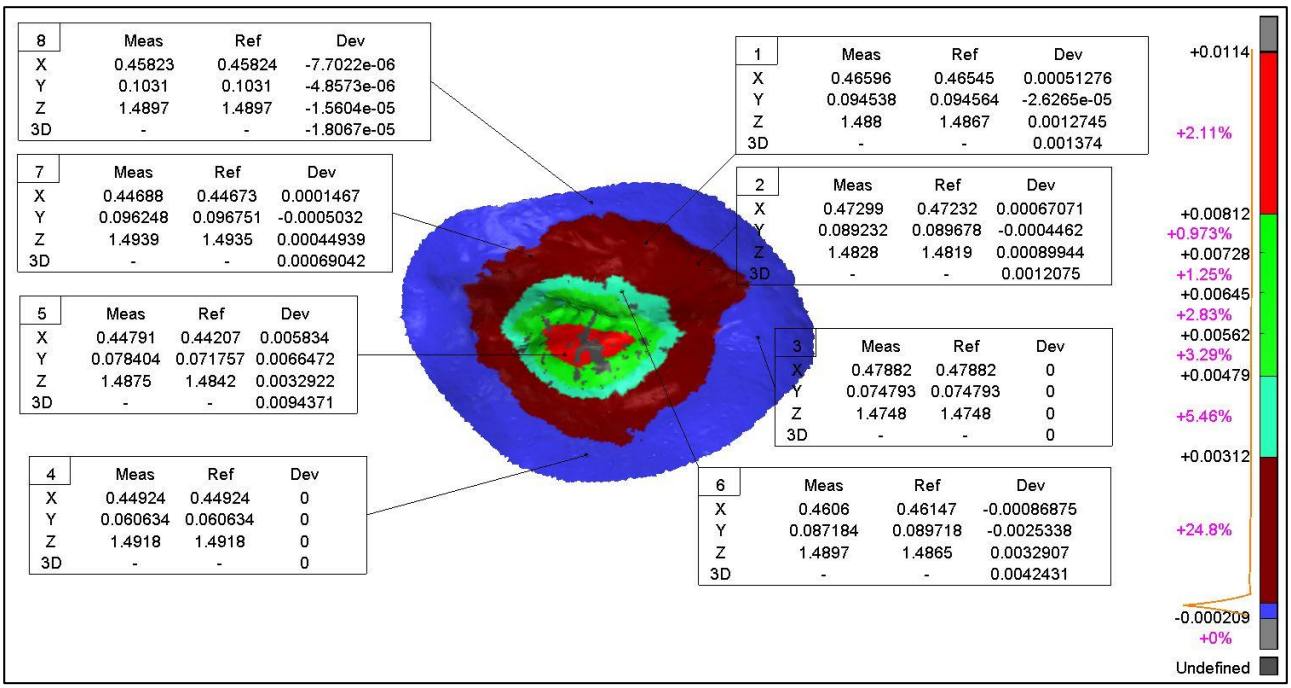

Figure 8. Color map displaying the result of the prosthesis matching inspection with the reference model.

3.3. Printing the Restored Model

Following the model slicing, a general-purpose resin material was used for printing the restored model as a prototype as shown in **Fig. 9,** left. The printing of the prototype took (6 h 45 m 57s) and consumed (9.6 ml) of the printing material. Then, the prototype was checked on the patient to detect incongruent margins. The matching result was acceptable, and the model does not need any correction, which indicates the digital workflow precision. Unfortunately, medical-made silicone material is not available to fabricate the eye prosthesis, characterized by purity, is highly biocompatible, heat resistant, and lasts, thus achieving safe contact with the patient's body. So, the steps of mold fabricating and silicone casting were avoided, and the rapid-prototyped model was relied on as the required prosthesis. To paint the RP model and get an orbital prosthesis as close to reality as possible, the color tone of the patient's skin was taken using skin tone papers. Then, the RP model was colored. **Fig. 9**, Right shows the final orbital prosthesis colored. While **Fig. 10** illustrates the final prosthesis on the patient.

In **Fig. 9,** left, it can be noticed that the model was printed with high-quality results. The main reason is using a smaller layer thickness in printing (0.05 mm). However, in **Fig. 9,** right, and **Fig. 10**, it can be noticed that the coloring process was not professional. This is due to a lack of coloring skills and requires people with high experience in texture coloring to deliver a more realistic product.

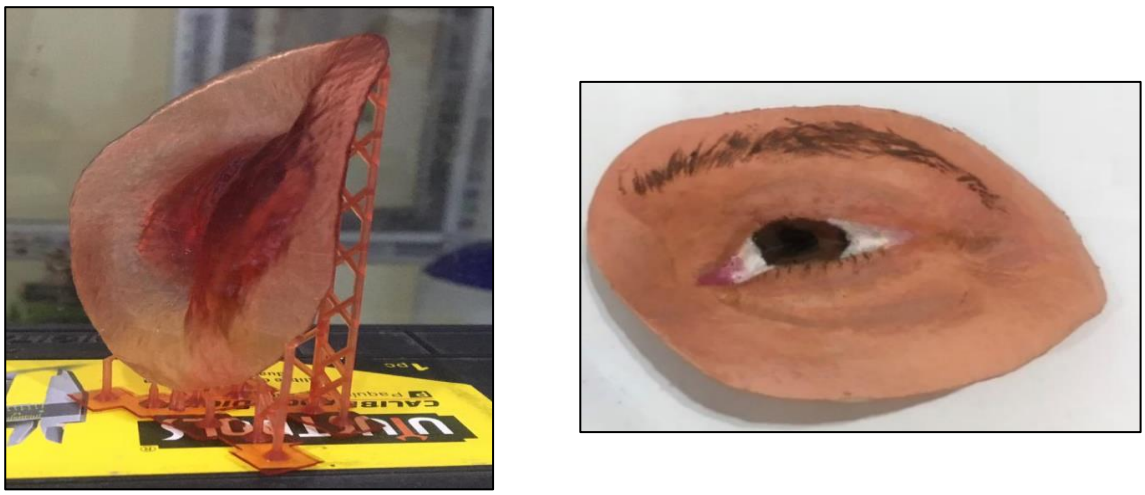

Figure 9. Restored printed model (eye prosthesis). (Left) before coloring. (Right) after coloring.

Figure 10. The final prosthesis on the patient.

4. CONCLUSIONS

Prosthetics extraction-based computer-vision photogrammetry represents a powerful alternative solution in the rehabilitation of maxillofacial deformities, especially when surgical intervention is difficult or not preferred. Through the recorded results, this approach provides a high-accuracy digital impression that is subsequently used in fabricating prostheses virtually using suitable CAD software. Also, it is considered a low-cost method and avoids the risk of exposure to harmful radiation or magnetic fields when using other sensors such as CT or MRI. The disadvantages of this method are that it requires data capturing skills and choosing the appropriate settings to process images and produce the 3D model, which may prompt the doctor to contract with specialists if he lacks this ability. Also, 3D printers may not be available to everyone, especially in developing nations.

On the other hand, many issues must be taken into consideration for future studies, such as designing a multi-camera rig surrounding the patient's head to reduce capturing time, collecting data consistency, and placing reference points with different depths on a fixed design frame with the patient face level to improve the evaluation process of the generated model. Also, selecting more study cases with various ages, genders, and deformations in the areas of the face is recommended. However, it can be claimed that the effectiveness of using the 3D-photogrammetry technique in maxillofacial rehabilitation is a noninvasive and low-cost technique.

5. STUDY LIMITATIONS

The limitation of this research is that the medical grade silicone used in casting the prostheses was not available, so the RP model made of resin material has been relied upon to test its suitability and to see the aesthetic of the prosthesis on the patient.

Acknowledgement

The authors gratefully acknowledge the case study patient who volunteered to participate in this research. Without her help and contribution, this work would never have been accomplished.

Author Contributions

Mohammed R. Falih undertook this research as part of his MSc studies at the College of Engineering/ University of Baghdad. This included the rehabilitation approach of the maxillofacial deformities and the Orbital Prosthesis prototyping to present alternative solutions to invasive approaches in biomedical Engineering applications. He also carried out the bulk of the manuscript preparation.
Fanar M. Abed supervised Falih's MSc research and guided the research development. She led earlier photogrammetry and laser scanning research at the College of Engineering at Baghdad University, which underpins the work reported herein. Abed contributed to the development, revision, and refinement of the manuscript.

Declaration of competing interest

The authors declare that they have no known competing financial interests or personal relationships that could have appeared to influence the work reported in this paper.

REFERENCES

Abbas, S.F. and Abed, F.M., 2024. Revolutionizing Depth Sensing: A Review study of Apple LiDAR sensor for as-built scanning Applications. *Journal of Engineering*, in press.

Abed, F.M., 2015. Digital Orthophoto Production Using Close-Range Photographs for High Curved Objects. *Journal of Engineering*, 21(3), pp.142–157. Doi: 10.31026/j.eng.2015.03.09.

Agisoft, 2021. *Agisoft Metashape User Manual: Professional Edition, Version 1.7*. [online] Available at: <https://www.agisoft.com/pdf/metashape-pro_1_7_en.pdf> [Accessed 3 Jun. 2021].

Ahmed, S., El-Shazly, A., Abed, F. and Ahmed, W., 2022. The Influence of Flight Direction and Camera Orientation on the Quality Products of UAV-Based SfM-Photogrammetry. *Applied Sciences (Switzerland)*, 12(20), p.10492. Doi: 10.3390/app122010492.

Alam, M.S., Sugavaneswaran, M., Arumaikkannu, G. and Mukherjee, B., 2017. An innovative method of ocular prosthesis fabrication by bio-CAD and rapid 3-D printing technology: A pilot study. *Orbit*, 36(4), pp.223–227. Doi: 10.1080/01676830.2017.1287741.

Bali, N., Dhall, R.S. and Singh, N., 2015. Various steps involved in fabrication of an ocular prosthesis: A case report. *Int J Dent Med Res,* 1(5), pp.93–96.

Ballo, A.M., Nguyen, C.T. and Lee, V.S.K., 2019. Digital Workflow of Auricular Rehabilitation: A Technical Report Using an Intraoral Scanner. *Journal of Prosthodontics*, 28(5), pp.596–600. Doi: 10.1111/jopr.13057.

Bi, Y., Wu, S., Zhao, Y. and Bai, S., 2013. A new method for fabricating orbital prosthesis with a CAD/CAM negative mold. *The Journal of Prosthetic Dentistry*, 110(5), pp.424–428.Doi: 10.1016/j.prosdent.2013.05.003.

Buzayan, M.M., Ariffin, Y.T., Yunus, N. and Mahmood, W.A.A.B., 2015. Ocular Defect Rehabilitation Using Photography and Digital Imaging: A Clinical Report. *Journal of Prosthodontics*, 24(6), pp.506–510. Doi: 10.1111/jopr.12235.

Cevik, P. and Kocacikli, M., 2019. Three-dimensional printing technologies in the fabrication of maxillofacial prosthesis : A case report. *The International Journal of Artificial Organs*, 43(5), pp.343–347. Doi: 10.1177/0391398819887401.

Chiu, M., Hong, S.C. and Wilson, G., 2017. Digital fabrication of orbital prosthesis mold using 3D photography and computer-aided design. *Graefe's Archive for Clinical and Experimental Ophthalmology*, 255(2), pp.425–426. Doi: 10.1007/s00417-016-3544-2.

Chunhua, S. and Guangqing, S., 2020. Application and Development of 3D Printing in the Medical Field. *Modern Mechanical Engineering*, 10(03), pp.25–33. Doi: 10.4236/mme.2020.103003.

Ciocca, L. and Scotti, R., 2014. Oculofacial rehabilitation after facial cancer removal: Updated CAD/CAM procedures. A pilot study. *Prosthetics and Orthotics International*, 38(6), pp.505–509. Doi: 10.1177/0309364613512368.

Difar, H.F. and Abed, F.M., 2022. Automatic Extraction of Unmanned Aerial Vehicles (UAV)-based Cadastral Map: Case Study in AL-Shatrah District-Iraq. *Iraqi Journal of Science*, 63(2), pp.877–896. Doi: 10.24996/ijs.2022.63.2.40.

Falih, M.R., Abed, F.M., Salazar-Gamarra, R. and Dib, L.L., 2021. Efficiency of +IDonBlender Photogrammetric Tool in Facial Prosthetics Rehabilitation – An Evaluation Study. *Karbala International Journal of Modern Science*, 7(4), pp.421–436. Doi: 10.33640/2405-609X.3167.

Gachake, A., Fulsundar, P. and Kadam, P., 2021. Prosthetic rehabilitation of a patient with acquired orbital defect using spectacle retained orbital prosthesis - A Case Report. *Journal of Prosthodontics Dentistry*, 16(2), pp.1–5. Doi: 10.1007/s13191-011-0093-6.

Goiato, M.C., de Caxias, F.P. and dos Santos, D.M., 2018. Quality of life living with ocular prosthesis. *Expert Review of Ophthalmology*, [online] 13(4), pp.187–189. Available at: <https://doi.org/10.1080/17469899.2018.1503534>.

Jamayet, N. Bin, Srithavaj, T. and Alam, M.K., 2013. A complete procedure of ocular prosthesis: A case report. *International Medical Journal*, 20(6), pp.729–730.

Karayazgan-Saracoglu, B. and Ozdemir, A., 2017. Fabrication of an Orbital Prosthesis Combined with Eyebrow Transplantation. *Journal of Craniofacial Surgery*, 28(2), pp.479–481. Doi: 10.1097/SCS.0000000000003319.

Kloc, B., Mazur, A. and Szumiło, M., 2021. Comparison of Free and Commercial Software in the Processing of Data Obtained from Non-Metric Cameras. *Journal of Ecological Engineering*, 22(2), pp.213–225. Doi: 10.12911/22998993/131074.

Lanzara, R., Thakur, A., Viswambaran, M. and Khattak, A., 2019. Fabrication of ocular prosthesis with a digital customization technique – A case report. *Journal of Family Medicine and Primary Care*, 8(3), pp.1239–1242. Doi: 10.4103/jfmpc.jfmpc_133_19.

Liu, H., Bai, S., Yu, X., and Zhao, Y., 2019. Combined use of a facial scanner and an intraoral scanner to acquire a digital scan for the fabrication of an orbital prosthesis. *The Journal of Prosthetic Dentistry*, 121(3), pp.531–534. Doi: 10.1016/j.prosdent.2018.05.019.

Maskey, B., Mathema, S.R.B., Shrestha, K. and Bhochhibhoya, A., 2019. A Simplified Approach to Fabricate a Hollow Ocular Prosthesis. *Journal of Prosthodontics*, 28(7), pp.849–852. Doi: 10.1111/jopr.12757.

Matsuoka, A., Yoshioka, F., Ozawa, S. and Takebe, J., 2019. Development of three-dimensional facial expression models using morphing methods for fabricating facial prostheses. *Journal of Prosthodontic Research*, 63(1), pp.66–72. Doi: 10.1016/j.jpor.2018.08.003.

Nalawade, T.M., Mallikarjuna, R.M., Anand, B.M., Anand, M., Shashibhusan, K. and Reddy, V.S., 2013. Prosthetic Rehabilitation of a Pediatric Patient with an Ocular Defect. *International Journal of Clinical Pediatric Dentistry*, 6(1), pp.62–65. Doi: 10.5005/jp-journals-10005-1190.

Pun, S.N., Shakya, R., Adhikari, G., Parajuli, P.K., Singh, R.K. and Suwal, P., 2016. Custom Ocular Prosthesis for Enucleated Eye: A Case Report. *Journal of College of Medical Sciences-Nepal*, 12(2), pp.78–80. Doi: 10.3126/jcmsn.v12i3.16018.

Reitemeier, B., Notni, G., Heinze, M., Schöne, C., Schmidt, A. and Fichtner, D., 2004. Optical modeling of extraoral defects. *The Journal of Prosthetic Dentistry*, 91(1), pp.80–84. Doi: 10.1016/j.prosdent.2003.10.010.

Salazar-Gamarra, R., Seelaus, R., Da Silva, J.V.L., Da Silva, A.M. and Dib, L.L., 2016. Monoscopic photogrammetry to obtain 3D models by a mobile device: A method for making facial prostheses. *Journal of Otolaryngology - Head and Neck Surgery*, 45(1), pp.1–13. Doi: 10.1186/s40463-016-0145-3.

Sarhan, H.R. and Abed, F.M., 2021. The Feasibility of Using UAV Structure from Motion Photogrammetry to Extract HBIM of the Great Ziggurat of UR. *Iraqi Journal of Science*, 62(11), pp.4518–4528. Doi: 10.24996/ijs.2021.62.11(SI).31.

Shamkhi, A. and Abed, F.M., 2020. *The fusion of laser scans and digital images for effective cultural heritage conservation*. The University of Baghdad.

Sharma, N., Thakral, G.K., Mohapatra, A., Seth, J. and Vashisht, P., 2014. A simplified technique for fabrication of orbital prosthesis. *Journal of Clinical and Diagnostic Research*, 8(6), pp.ZD10–ZD12. Doi 10.7860/JCDR/2014/9246.4490.

Shrivastava, K.J., Shrivastava, S., Agarwal, S. and Bhoyar, A., 2015. Prosthetic rehabilitation of large mid-facial defect with magnet-retained silicone prosthesis. *Journal of Indian Prosthodontist Society*, 15(3), pp.276–280. Doi: 10.4103/0972-4052.161571.

Singh, R., Dua, P., Prakash, P. and Bhandari, S.K., 2019. Rehabilitation of an Orbital Defect with Silicone Orbital Prosthesis: A Case Report. *International Journal of Contemporary Medical Research [IJCMR]*, 6(11), pp.16–19. Doi: 10.21276/ijcmr.2019.6.11.30.

Weisson, E.H., Fittipaldi, M., Concepcion, C.A., Pelaez, D., Grace, L. and Tse, D.T., 2020. Automated Noncontact Facial Topography Mapping, 3-dimensional Printing, and Silicone Casting of Orbital Prosthesis. *American Journal of Ophthalmology*, 220, pp.27–36. Doi: 10.1016/j.ajo.2020.06.032.

Yadav, S., Narayan, A.I., Choudhry, A. and Balakrishnan, D., 2017. CAD/CAM-Assisted Auricular Prosthesis Fabrication for a Quick, Precise, and More Retentive Outcome: A Clinical Report. *Journal of Prosthodontics*, 26(7), pp.616–621. Doi: 10.1111/jopr.12589.